Transactions, SMiRT-24
BEXCO, Busan, Korea - August 20-25, 2017
Division I

A STUDY OF FRACTURE PROPERTIES OF HIGH ALUMINA SHIELDING CONCRETE (HASC)

Yu-Cheng KAN[1], Kuang-Chih Pei[2], Meng-Hwa Cheng[3]

[1] Associate Professor, Dept. of Construction Engineering, Chaoyang University of Technology, Taiwan
[2] Senior engineer, Institute of Nuclear Energy Research, Taiwan
[3] Research assistant, Dept. of Construction Engineering, Chaoyang University of Technology, Taiwan

ABSTRACT

Concrete is widely used as a shielding material of nuclear facilities for radiation protection in virtue with its high content of hydrogen which can slow down the thermal neutrons. In order to strengthen the shielding performance as well as mechanical property, the concrete often includes some specific aggregates with higher specific gravity ranging from 2.5 to 7.8. This study attempts to adopt the shielding materials commonly used in aerospace industry -alumina oxide (Al_2O_3) and boron carbon (B_4C) in concrete to enhance the shielding ability. The mechanical properties and fracture toughness of this type of concrete will be presented. The concrete mixtures included high alumina cement, B_4C of 11% by weight of cement, and Al_2O_3 inclusions of 20%, 40%, 60%, irrespectively, of fine aggregate replacement. The mechanical properties and the fracture toughness of high alumina shielding concrete (HASC) and normal concrete (NC) were investigated and compared. The results showed that HASC concrete had high strength in the early stage, but the tensile strength and the compressive strength decreased with time duration. In addition, the tensile strength and the fracture toughness decreased as the alumina oxide increased, which can be attributed to the conversion effect.

INTRODUCTION

In nuclear engineering, heavy concrete is used in biological shields or in shielding walls in a reactor vessel, as shown in Figure 1. Deterioration of the heavy concrete, either cracking or degradation, may lead to leakage of radiation and is attractive to civil engineers since who have elucidated more of the mechanics of concrete and have figured out more relevant technology. The ACI Manual of Concrete Practice specifies thorough procedures for measuring, mixing, transporting and placing. Typical unit weights and compressive strengths of heavy concrete with various types of aggregates are also provided. Yet, little information on other mechanical properties and fractures has been reported. Kan and Pei (2004) have found that the compressive and tensile strengths of heavy concrete did not differ from those of regular mortar at the same water to cement ratio; however, the modulus of elasticity increases with the heavy aggregate aggregates. Kan and Yang (2012) later also investigated the toughness of heavy concrete strengthened by the inclusion of steel fibers. Recently, Kinno et al. (2007) has attempted to develop many mixtures of low-activation concrete and reported that the concrete including fused alumina aggregate and high alumina cement contribute led to the least activation among all the designated mixtures. Thus, it seems reasonable and necessary to access the feasibility to use this type of material in shielding structure design. Thus, the research investigated many engineering properties and strengths of low-activated concrete influenced by the various aggregates of high aluminum inclusion.

As far as environmental protection is concerned, more efforts must be made to advance inspection techniques and assess repairs of shielding structures. Accordingly, the fracture characteristics which can

reflect inside structural behaviour and may be related to the residual strength of HASC structure must be figured out.

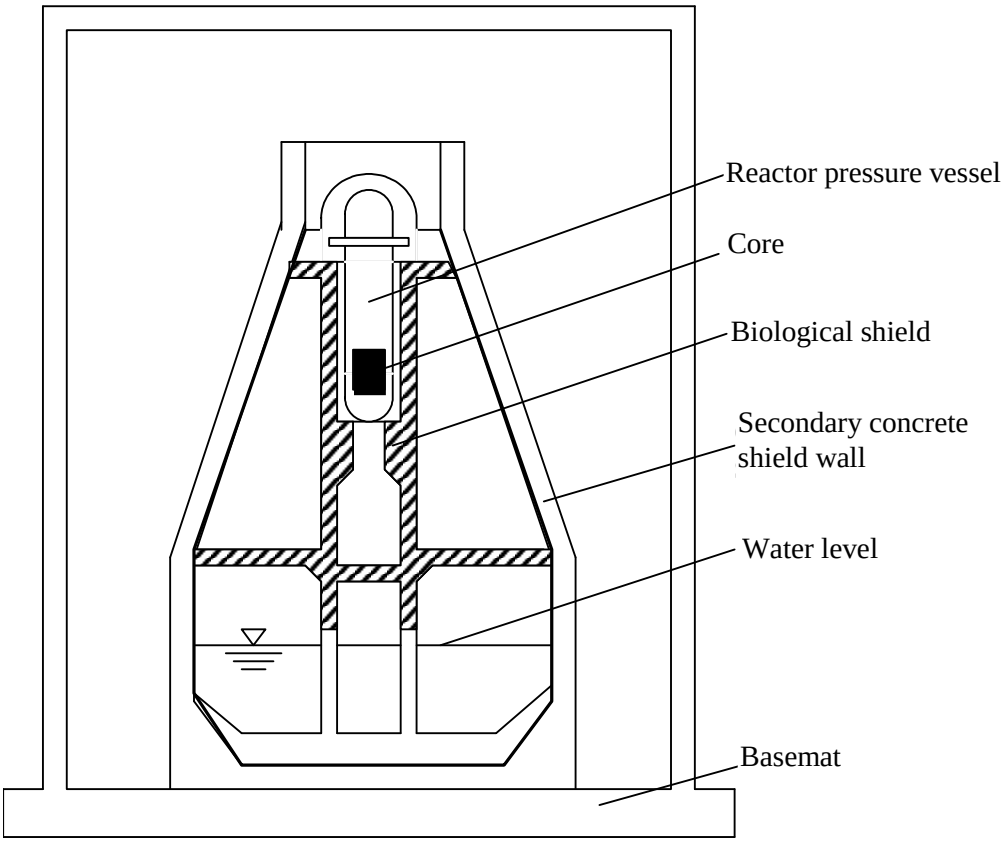

Figure 1. A schematic sketch of BWR concrete containment.

Conversion of High Alumina Concrete

Conversion is the result of the hydration products which change from metastable phases to more stable phases. It is apt to take place in the hydration of calcium aluminate cement (CAC). Once converted, the more stable hydration products form a smaller crystalline structure and take up less space, increasing the porosity of the overall matrix and consequently reducing the strength. The strength loss occurs depending primarily on the temperature of the concrete during both in hydration and in service as well as the presence of moisture. This process can range from hours to many years.

Hydration and Conversion of CAC

Heidelberger Zement (1998) has reported that The hydration process in calcium aluminate cement (CAC) systems is different from that of Portland cement (PC) systems. Hydration is the reaction between cement and water. In General, 60-80% of hydration of Portland cement (PC) occurs in 28 days depending on the type of PC, and the hydration will still slowly proceed after 28 days. However, most of the hydration in CAC occurs only within the first 24 hours. In fact, when CAC is mixed with water, a small quantity of heat is liberated within minutes. Then no hydration occurs throughout almost 2-3 hours, which is called as dormant period. After the dormant period, CAC reacts with almost all of the water very rapidly and almost complete hydration is realized within 24 hours, accompanied by a large amount of heat generation. This summarizes also the distinct property of CAC, slow setting and rapid hardening.

Hydration Mechanism of CAC

Garsel (1996) reported that the hydration of CAC starts by dissolving of clinker minerals in water as calcium ions and aluminium hydroxide, which continues till the saturation level. It is followed by nucleation and precipitation of calcium aluminate hydrate crystals and gibbsite (AH_3). These hydrate crystals start to precipitate close to the unreacted clinker surface by forming a gel layer. Fujii et al. (1990) reported that this layer is permeable to water. Therefore, further hydration of the underlying clinker grains takes place easily as a continuous process as long as enough water for dissolution and hydration is available.

Table 4: Physical Properties of Calcium Aluminate Hydrates. (Garsel, 1996)

Hydration Products	Chemical Composition (%)			Crystal Form	Density (g/cm^3)	Volume Ratio of Hydrates to CA
	CaO	Al_2O_3	H_2O			
CAH_{10}	16.6	30.1	53.3	Metastable hexagonal prism	1.72	3.68
C_2AH_8	31.3	28.4	40.3	Metastable hexagonal plates	1.95	2.33
C_3AH_6	44.4	27.0	28.6	Stable cubic trapezohedrals	2.52	1.75
AH_3	-	65.4	34.8	Stable hexagonal prism	2.42	-

At initial stages, hydration crystals form a gel layer coating the unreacted grains. The mix is still plastic. Depending on the progress in crystal formation as a result of continuous dissolving precipitation, some bonds take place among clinker grains, resulting in stiffening of the mix. As hydration proceeds further, the mix gets stiffer by gaining strength. Finally, the final stable structure is formed when the water is used up and no further hydration crystal grows.

Fracture Mechanics of Concrete

Cracks always occur before a concrete structure deteriorates or fails. The study of cracks in concrete is referred to as concrete fracture mechanics, initiated by Kaplan (1961). A crack in concrete is thought to begin when the fracture toughness that is always defined quantitatively in terms of critical stress intensity factor, K_C, or the fracture energy, G_C, has been exceeded. Much research has addressed the fracture toughness of normal concrete with various mixtures (Naus, 1969), but little research has addressed the strength and fracture properties of heavy concrete. A fracture process zone exists in front of the tip of a propagating crack. A number of proposals have recently been suggested to RILEM (1989), such as Hillerburg's fracture model (1985), Bazant's size effect model (1986), Jenq and Shah's two-parameter model (1985) and Karihaloo and Nallathambi's effective crack model (1991), all of which provide methods for determining the fracture properties of concrete.

For concrete structures such as reactor containment, crack inspection on concrete becomes a critical item for extending the operating license of in-service reactor. A typical example is the Crystal River containment crack, which attracted more attentions and caused a great number of technical discussions. The fracture toughness of concrete which deals with the occurrence of cracks seems significant and necessary to be accessed in fracture mechanics manner before design and construction. This work

investigates the mixture, fabrication and many basic engineering properties of HAS concrete, including strengths and fracture toughness under the influence of varying contents of aluminate inclusions. The fracture properties, especially, fracture toughness K_{IC}, will be a significant parameter in future work in conducting a fracture analysis based on finite element simulation for a shielding structure.

TESTING PROGRAM

Materials

A Type I Portland cement and an aluminate cement supplied by Kerneos Inc. in France were used in this study. The typical constituents of both cements are shown in Table 1.

Table 1: Constituents of cements.

Composition	Type I	HAC
Al_2O_3	4.95	50.8-54.2
CaO	61.96	35.9-38.9
SiO_2	20.42	4.5-5.6
Fe_2O_3	3.09	1.0-2.2
MgO	3.29	<1.0
TiO_2	-	<4.0

High alumina cement

In high alumina cement, the predominant compounds are calcium aluminates; calcium silicates account for no more than a few percent. The calcium aluminates react with water and the primary product is calcium aluminate decahydrate (CAH_{10}) which has essentially a hexagonal crystal form. This material is unstable and changes to tricalcium aluminate hexahydrate (C_3AH_6) spontaneously. The process occurs at room temperature and is accelerated by an increase in temperature. The effect of conversion, as it is known, is accompanied by an increase in porosity and a decrease in strength.

Fused alumina aggregates

Unlike normal concrete, the main feature of heavy concrete is the inclusion of metallic fillers, which are usually ilmenite, limonite-goethite, serpentine, magnetite, barite, ferrophosphorous, steel aggregate and iron shot. In this study, fused aluminate aggregates with 95% inclusion of Al_2O_3 were used as part of fine aggregates replacement in concrete. It has an average grain size of 1 mm (ANSI No. 20) with a specific gravity is 3.90 and a hardness of 9 in Moh's scale.

Boron carbide

The ability of boron carbide to absorb neutrons without forming long-lived radionuclides makes it attractive as an absorbent for neutron radiation arising in nuclear power plants. Nuclear applications of

boron carbide include shielding, control rod and shut down pellets. Within control rods, boron carbide is often powdered, to increase its surface area. In this study, boron carbide powder was used as part of concrete inclusion. It has an average grain size of 0.045 mm (ANSI No. 240) with a specific gravity is 2.52 and a hardness of 9.6 in Moh's scale.

Table 2: Concrete mixtures.

	NC	HAC		
Component		20%	40%	60%
Water	193§	196	200	204
Cement	386	353	361	368
Aggregate	995	1012	1032	1054
Sand	762	619	474	322
B_4C	-	39	40	41
Al_2O_3	-	155	316	484
U.W.	2336	2375	2423	2473

§All units are in kg/m^3. *Type I Portland cement concrete;
**high aluminum concrete.

Concrete Mixtures

Table 2, have a water/cement ratio of 0.5. The amount of boron carbide B_4C is fixed at 10 % by weight for all HASC mixtures; while the amount of Al_2O_3 aggregates is varied. The low-activated concretes were designated with 20 %, 40 % and 60 % fine aggregate replacement by fused aluminum oxide (Al_2O_3 aggregates) by weight, to examine the effect of the high alumina cement and various amounts of Al_2O_3 aggregates on the mechanical properties of HASC. The HAS concrete mix with 40% sand replacement by Al_2O_3 aggregates, for example, is specified as HASC40. It is noted that the unit weight of concrete increases with the Al_2O_3 aggregates, as shown in Table 2. And, it is found that the placement in concrete with 60% of Al_2O_3 aggregates by weight produced a harsh mix in workability. The mechanical properties of both HASC and normal concretes were tested and compared.

Mixing and Curing

The procedure for mixing HASC is a bit different to that for conventional concrete. Fused alumina aggregates and boron carbide were used as part of replacements of fine aggregates and cement, irrespectively. In a typical mixing procedure, all aggregates were mixed first in a mixer, followed by alumina cement and cold water (with a temperature under 20°C). However, an excess compacting vibration must be avoided to prevent segregation of fused aluminate aggregates due to its high specific gravity. In addition, the work duration for HAS mix is quite shorter than regular concrete and has to affirm sufficient time for good workability in placing and casting. All concrete specimens were cast in molds. The normal concrete specimens were cured for one day and placed in water for 28 days prior to testing; while the HASC specimens were demolded after one hour for early strength gain measurements.

Testing Specimens

Three types of specimens made from the above four mixtures were fabricated in this testing program. The ϕ10 × 20 cm cylinders were used to determine the fundamental mechanical properties of concrete complying to ASTM Specifications, including the strengths, modulus of elasticity and wave velocity. The ϕ10 × 20 cm cylinders were primarily tested for compressive strength and tensile strength. A single-edge-notched beam type recommended by the RILEM, with the size of 10 × 10 × 45 cm and a span to depth ratio of four, was fabricated and tested as depicted in Figure 2 to obtain the fracture toughness.

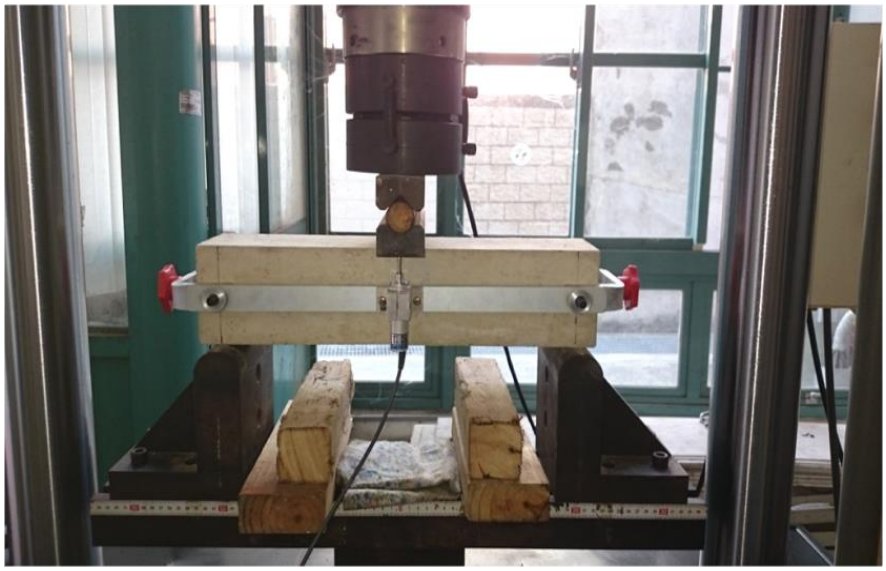

Figure 2. Configuration of Three-point bending test in MTS.

Evaluation of Fracture Toughness

Fracture toughness, in terms of the stress intensity factor, is determined following the method suggested by Karihaloo and Nallathambi (1991) in which single-notched beams are tested in three-point bending on a universal testing machine. A notch of 2 mm wide and one-third the beam depth is pre-cast on the middle for each beam as a crack starter which initiates the crack from the tip of notch. Load and displacement data are simultaneously recorded before the peak load is reached. Only the part of the curve that precedes the peak need to be considered and no softening curve is required. The formula for the critical stress intensity factor, K_{IC}, is,

$$K_{IC}^{e} = \sigma_n \sqrt{a_e} F(\alpha) \tag{1}$$

in which, σ_n is normal stress and

$$F(\alpha) = \frac{1.99 - \alpha(1-\alpha)(2.15 - 3.93\alpha + 2.70\alpha^2)}{(1+2\alpha)(1-\alpha)^{3/2}} \tag{2}$$

where $\alpha = a_e / W$ is the ratio of the critical effective crack depth to the beam depth and can be determined from the following formula.

$$\frac{a_e}{W} = \varepsilon_1 \left(\frac{\sigma_n}{E}\right)^{\varepsilon_2} \left(\frac{a_p}{W}\right)^{\varepsilon_3} \left(1 + \frac{g}{W}\right)^{\varepsilon_4} \tag{3}$$

In the above expression, ε_1, ε_2, ε_3 and ε_4 are coefficients of regression calibrated using experimental data, with a notch depth of a_p, and a grain size, g. Furthermore, the modulus of elasticity, E, is determined from a cylinder test.

Results and Discussion

The fundamental mechanical properties of concrete including compressive strength, splitting tensile strength and elastic modulus are presented in Table 3 and discussed as following.

Table 3: Mechanical properties of concrete

Mixture	day	f_c' (MPa)	f_t' (MPa)	E_c (GPa)
NC	28	30.1	3.04	21.7
	91	38.0	3.60	18.8
HASC20	28	43.7	3.72	26.3
	91	35.9	3.63	18.7
HASC40	28	50.2	3.69	26.4
	91	51.9	2.87	25.3
HASC60	28	44.3	3.10	28.1
	91	31.1	2.04	25.5

Compressive Strength

The compressive strength of HASC exceeds that of normal concrete and increases with Al_2O_3 aggregates for a given water/cemnt ratio. The compressive strengths for all mixes are shown in Figure 3. It reveals that an increase of Al_2O_3 aggregates causes the increase in the compressive strength. However, the mixture with an inclusion of 60% of Al_2O_3 aggregates by weight turns out lower compressive strength and can be attributed to the bad workability for placing the concrete. The mixture with 40% of Al_2O_3 aggregates appears the highest strengths in all the curing duration. The compressive strength of HASC turns out higher in its earlier age (before 7 days of curing), but decays later due to the effect of conversion.

Wave Velocity

The mechanical properties of concrete can be estimated from its wave velocity by means of ultrasonic equipments. The test results revealed that the wave velocity of HASC increases as the Al_2O_3 aggregates increases, as shown in Figure 4, which show a consistence with that of compressive strength of HASC. The mixture with 60% of Al_2O_3 aggregates by weight turns out the lower wave velocity and can be still attributed to the bad workability in placing the concrete. The mixture with 40% of Al_2O_3 aggregates appears the highest wave velocity before 28 days of curing duration. Notice that the wave velocity of all mixtures of HASC turn out decay in 91 day, which can be explained by the conversion effect.

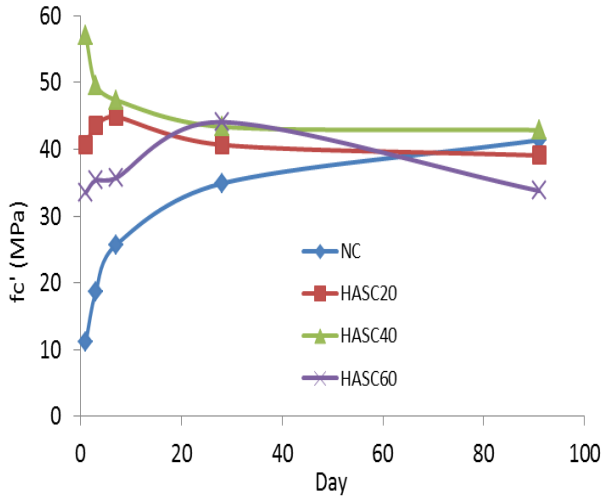

Figure 3. Compressive strength of concretes.

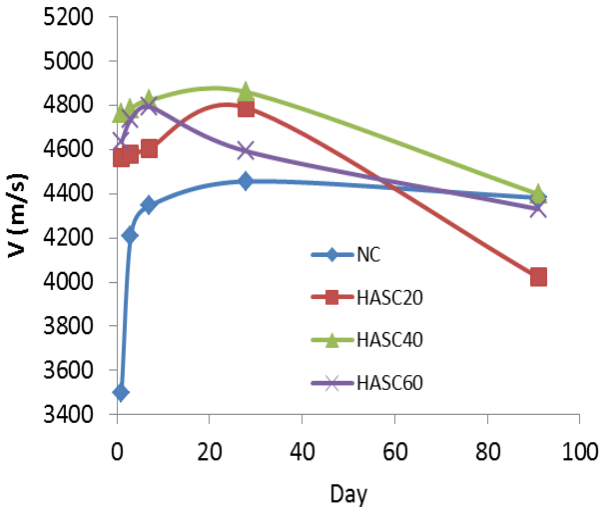

Figure 4. Wave velocity of concrete.

Splitting Tensile Strength

The splitting test was used to determine the tensile strengths of concrete with various amounts of Al_2O_3 aggregates. Figure 5 shows that the tensile strength of NC is lower than HASC in 28 days, but becomes higher in 91 days of age. Furthermore, the tensile strength of HASC decreases as the Al_2O_3 aggregates increase. Obviously, the voids resulted from conversion dominate the tensile strength of HASC. The tensile strength reduces in 91 days of curing duration and decays more severe as the Al_2O_3 aggregates increases.

Elastic Modulus

Test results showed that the modulus of elasticity of HASC exceeds that of normal concrete and increases with Al_2O_3 aggregates for a given water/cemnt ratio. Figure 6 reveals that an increase in Al_2O_3 aggregates causes an increase in the elastic modulus, which appears consistent with that of compressive strength.

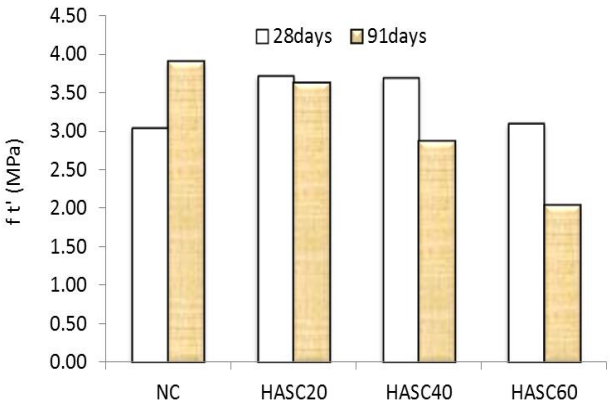

Figure 5. Tensile strength of concretes.

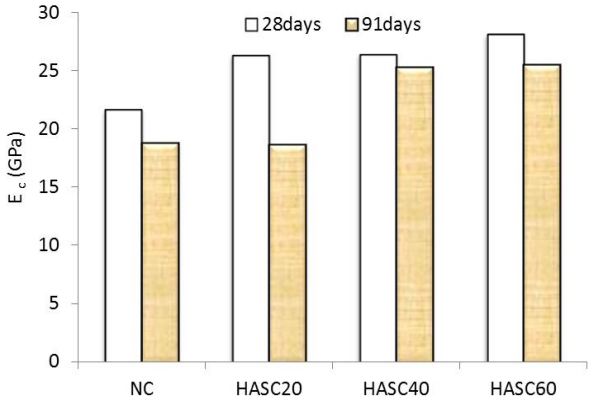

Figure 6. Elastic moduli of concretes.

Fracture Toughnesss

Fracture toughness, in terms of the stress intensity factor, is determined following the method suggested by Karihaloo and Nallathambi in which single notched beams are tested in three-point bending on a MTS testing system as shown in Figure 2. Load and displacement data are simultaneously recorded before the peak load is reached. Figure 7 shows that the fracture toughness K_{IC} of NC is much lower than HASC in 28 days, but becomes higher in 91 days of age. In addition, the K_{IC} of HASC decreases as the Al_2O_3 aggregates increases.This shows the same trend as that of tensile strength, which was dominated by the voids coming from the effect of conversion.

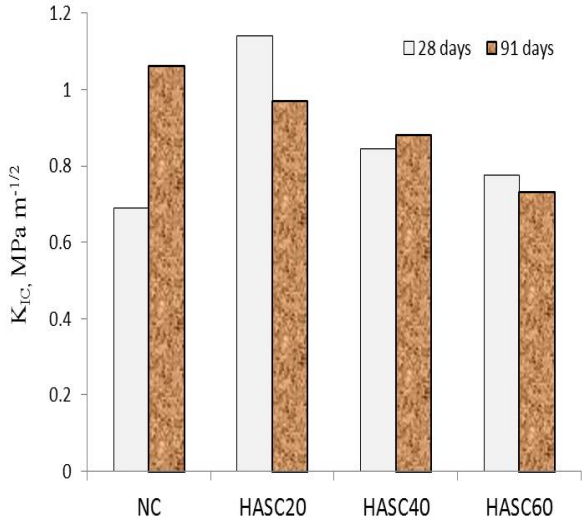

Figure 7. Fracture toughness of concretes.

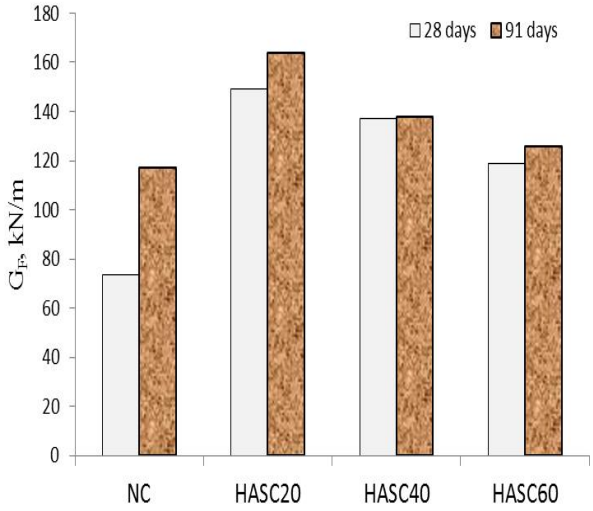

Figure 8. Fracture energy of concretes.

Fracture Energy

In Figure 8, the fracture energy G_F evaluated by Hillerborg's method shows that HASC has higher fracture energy G_F than that of normal concrete for a given water/cement ratio. However, the fracture energy seems to decrease with the increase of Al_2O_3 aggregates. And, the fracture energy in 91 days appears a bit higher than that in 28 days.

CONCLUSION

High alumina shielding concrete has higher compressive strength than normal for a given water/cement ratio. The compressive strength seems to be higher in the earlier age and decays after 7 days of curing. Concrete including 40% of Al_2O_3 aggregates as sand replacement performs the highest strength and workability as well. Elastic modulus of concrete appears to increase with the Al_2O_3 inclusion. The tensile strength, the fracture toughness and fracture energy seem to be decreasing with the increase of Al_2O_3 aggregates in concrete. The voids due to the effect of conversion do affect the mechanical properties of concrete.

ACKNOWLEDGEMENT

This research was supported by the Ministry of Science and Technology of Taiwan under the Grant MOST103-2211-E-324-035, which is sincerely grateful.

REFERENCES

ACI Manual of Concrete Practice (1989). Heavyweight Concrete – Measuring, Mixing, Transporting and Placing. Part II, 304.3R.

ASTM Standards C39-86, 1986. Test Method for Compressive Strength of Cylindrical Concrete Specimens.

ASTM Standards C496-87, 1987. Test Method for Splitting Tensile Strength of Cylindrical Concrete Specimens.

ASTM Standards C469-87, 1987. Test Method for Static Modulus of Elasticity and Poisson's Ratio of Concrete in Compression.

Bazant, Z.P., Kim, J.K. and Pfeiffer, P. A. (1986). "Determination of Fracture Properties from size effect Tests." *Journal of Structural Engineering*, ASCE, 112(2), 289-307.

Heidelberger Zement AG (1998). High Alumina Cement, Betoniek.

Cook, R. D., Malkus, D. S., Plesha, M. E. and Witt, R. J. (2002). *Concepts and Applications of Finite Element Analysis, 4th ed*., John Wiley & Sons.

Fujii, K., Kondo, W., Ueno, H., (1990). "Kinetics of Hydration of Monocalcium Aluminate", *Journal of American Ceramic Society*, Vol. 69 [4], pp. 623-635.

Garsel, D.V., (1996). *High Alumina Cements and Chemical Binders*, Seminar Given by Alcoa Industrial Chemicals Europe at Institute of Refractories Engineering, South Africa.

Hillerborg, A. (1985). The theoretical Basis of a Method to Determine the Fracture Energy G_F of Concrete. Materials and Structures 18(106), 291-296.

Hughes, T. J. R. and Allik, H. (1969) "Finite Elements for Compressible and Incompressible Continua," *Proc., Symposium on Application of Finite Element Methods in Civil Engineering*, ASCE, Nashville, TN, 27-62.

Jenq, Y.S. and Shah, S.P. (1985). Two Parameter Fracture Model for Concrete. *Journal of Engineering Mechanics*, ASCE, 111(10), 1227-1241.

Kan, Yu-Cheng, K.- C. Pei and C.-L. Chang (2004) "Strength and Fracture Toughness of Heavy Concrete with Various Iron Aggregate Inclusions, *J. Nuclear Engineering Design*, 228, 119-127.

Kan,Yu-Cheng, Hsuan-Chih Yang and Kuang-Chih Pei, Adv Mat Res, 512 - 515, pp. 2908 – 13 (2012)

Kaplan, M.F. (1961). Crack Propagation and the Fracture of Concrete. *Journal of the American Concrete Institute*, 58(5), 591-610.

Karihaloo, B.L. and Nalathambi, P. (1991). Notched Beam Test: Mode I Fracture Toughness. in RILEM Report 5, Fracture Mechanics Test Methods for Concrete, Edited by Shah, S.P., and Carpineteri, A., Chapman & Hall, London, 1-86.

Kinno, Masaharu, et al. (2011). "Low-Activation Multilayer Shielding Structure of Light Water Reactor Using Various Types of Low-Activation Concrete," *Progress in Nuclear Science and Technology*, 128-31.

Kinno, Masaharu, et al. (2007) "Low-Activation Reinforced Concrete Design Methodology (10)-Low-Activation Concrete Based on Fused Alumina Aggregates and High Alumina Cement," Proceeding, SMiRT 19, Toronto.

Lessing, P. (2008). Developments in the Formulation and Reinforcement of Concrete, Sidney Mindess.

Marsden, B. J. and Hall, G. N. (2012) "Graphite in Gas-cooled Reactors," *Comprehensive Nuclear Materials*, Elsevier, UK.

Malhotra, V.M. and Carino, N.J. (1991). CRC Handbook on Nondestructive Testing of Concrete, CRC Press, Inc.

Naus, D.J. and Lott, J.L. (1969). Fracture Toughness of Portland Cement Concretes. *ACI Journal*, , 66(6), 481-489.

Prinja, N. K., Shepherd, D., Curley, J. (2005). "Simulating structural collapse of a PWR containment," *Nuclear Engineering and Design*, UK, 230, 2033-2043.

RILEM 89-FMT (1990). Determination of Fracture Parameters (K_{IC}^S and $CTOD_C$) of Plain Concrete Using Three-Point Bend Tests. Materials and Structures, 23(138), 457-460.